

Momentum-transfer dependence of the K absorption edge of lithium

J. J. Ritsko, S. E. Schnatterly, and P. C. Gibbons

Joseph Henry Laboratories of Physics, Princeton University, Princeton, New Jersey 08540

(Received 24 June 1974)

The lithium K absorption edge has been studied as a function of momentum transfer in a high-resolution inelastic-electron-scattering experiment and found to exhibit no significant change with momentum transfer up to 1.2 \AA^{-1} . This result places severe restrictions on theories which interpret the shape of the threshold in terms of the final-state electron-hole interaction, and compatibility with this experiment could only be obtained in such theories by the utilization of a range ($\xi < 0.01 \text{ eV}$) or an s -wave phase shift ($\delta_0 < 0.5$), values which differ from the presently accepted calculations. Our results are consistent with an edge shape determined by a simple step function in the one-electron transition probability convoluted with broadening due to phonon or lifetime effects.

I. INTRODUCTION

Theories which attempt to calculate soft-x-ray emission and absorption spectra in metals fall into two camps. There are those which maintain that the dominant effect at threshold is the electron-hole interaction, often resulting in an excitonic-like enhancement of the absorption edge. Others maintain that properly calculated one-electron transitions neglecting this interaction are sufficient. We have performed an experiment which should clearly distinguish between these competing theories.

The idea of possible excitonic effects at x-ray thresholds was first proposed by Mahan¹ and later greatly embellished by Nozières and co-workers.²⁻⁴ Relying on a detailed perturbation-theory calculation of the final-state conduction-electron-core-hole interaction, Nozières and co-workers confirmed the earlier prediction of Mahan and cast the theory in its presently accepted form. Near threshold the x-ray absorption or emission rate S has the form⁴

$$S \approx \sum_{l,m} |W_{l,m}|^2 \left(\frac{\xi}{E_f - E_0} \right)^{\alpha_l}. \quad (1)$$

Here $W_{l,m}$ is the one-electron x-ray transition matrix element coupling the core state to the partial wave (l, m) of the conduction-state wave function. E_0 is the experimentally determined threshold energy. ξ (which we refer to as the range parameter) is a constant thought to be of the order of the Fermi energy. E_f is the conduction-state energy. The exponents α_l can be calculated from the scattering phase shifts δ_l associated with the scattering of Fermi-surface electrons from the potential of the deep core hole⁴

$$\alpha_l = \frac{2\delta_l}{\pi} - 2 \sum_l (2l+1) \left(\frac{\delta_l}{\pi} \right)^2. \quad (2)$$

These phase shifts are related by the Friedel sum rule⁵

$$\sum_l (2l+1) \delta_l = \frac{\pi}{2}. \quad (3)$$

In the first of many model calculations Ausman and Glick⁶ calculated the scattering phase shifts which would arise from a screened Coulomb potential. Their results for lithium and sodium were nearly identical: $\delta_0 \approx 1$, $\delta_1 \approx 0.15$, and $\delta_2 \approx 0.02$, all other phase shifts being smaller still. Using these phase shifts and the theory of Nozières *et al.* they deduced $\alpha_0 \approx 0.4$ and $\alpha_1 \approx -0.1$ for both lithium and sodium (all other α 's being about -0.2). These results are in qualitative agreement with experiment since the $L_{2,3}$ threshold in Na appears quite peaked, and the K edge of Li is rounded. $L_{2,3}$ thresholds should be peaked because the electric dipole operator selects the s -wave part of the plane-wave-like conduction states near the Fermi energy, and α_0 is positive. Similarly, dipole transitions from K shells are made to p -like conduction states and are rounded since α_1 is negative.

Several other calculations of these phase shifts have been made, all in reasonable agreement with those above. Mahan⁷ has used a Fredholm-type method due to Noyes which yields essentially the same δ_l 's. More recently, Longe⁸ has used a Thomas-Fermi potential, an Ashcroft pseudopotential, a modified Ashcroft pseudopotential, and an orthogonalized-plane-wave (OPW) method to determine the phase shifts. He considers his OPW method the more accurate, with the results $\delta_0 = 0.70$ and $\delta_1 = 0.14$. Mahan⁹ has also recently calculated the phase shifts using the Heine-Abrankov model potential. His results for lithium are in excellent agreement with the values of Ausman and Glick, although for sodium he obtains a somewhat smaller s -wave phase shift.

The above theoretical picture has recently been questioned by Dow and co-workers, who maintain that the apparent agreement with experimental results is misleading and inconsistent. In a series

of papers¹⁰⁻¹³ they suggest that the shape of the K edge in Li is due to phonon broadening, that the K and $L_{2,3}$ edges in aluminum do not fit the final-state interaction-theory prediction, and that in other simple metals exponents derived from experimental data do not agree with the theoretical calculations.

The principal alternative to the theory of Mahan and Nozières is that simple one-electron band structure with properly calculated transition matrix elements and density of states is the dominant factor at x-ray thresholds. Although the band structure and density of states for the conduction band of lithium was calculated in great detail by Ham,¹⁴ a precise calculation of the soft-x-ray emission and absorption spectra was made by McAlister.¹⁵ He showed that the shape of both emission and absorption thresholds could be explained entirely in terms of one-electron band theory if a Gaussian broadening function were convoluted with the theoretical spectra. This broadening was presumed to be due to phonons.

The difficulty in determining the detailed shape of the x-ray threshold in lithium is that both one-electron band theory and the final-state interaction theory predict an absolutely sharp threshold, whereas in reality the threshold is broadened. This broadening could be due to many effects, the principal ones of which are thermal smearing of the Fermi energy, phonon modulation of the core level, and lifetime broadening. Thermal smearing of the Fermi energy should be small (~ 0.06 eV at 300°K) and easily calculated. Direct phonon coupling of the core state to the lattice should produce a broadening with full width at half-maximum (FWHM) of 0.1 eV in lithium at 300°K .¹⁶ Dow *et al.*¹⁰ have argued that an indirect coupling of the core state to the lattice via the conduction electrons could result in additional phonon broadening with FWHM of 0.46 eV, although a detailed calculation has not yet been shown. Lastly, the lifetime of the core hole in Li has recently been calculated.¹⁷ The Auger decay rate for the $1s$ hole in lithium was found to be significantly larger than for other low- Z elements and should contribute significantly to the observed edge broadening.

In the case of Li the basic question is this: Regardless of phonon or lifetime broadening, is there any evidence that the final-state electron-hole interaction influences the shape of the K edges of lithium? Recently an experiment was proposed by Doniach, Platzman, and Yue¹⁸ which would discriminate between the competing pictures of the threshold shape. They proposed an inelastic hard-x-ray scattering experiment in which the absorption threshold should change dramatically as a function of momentum transfer if the dominant process at threshold were the final-state conduction-electron-core-hole interaction. The scattering cross sec-

tion per unit energy loss per unit solid angle for inelastic x-ray scattering is¹⁸

$$\frac{d^2\sigma}{dE d\Omega} \propto \sum_f \langle \psi_f | \sum_j e^{i\vec{q}\cdot\vec{r}_j} | \psi_i \rangle|^2 \delta(E_f - E_i - E), \quad (4)$$

where ψ_i , ψ_f are the initial- and final-state many-electron wave functions with energies E_i , E_f . \vec{q} is the momentum transfer and \vec{r}_j is the position of the j th electron in the solid. Doniach *et al.* showed that the theory of Nozières *et al.* applied to x-ray scattering could be cast in the form

$$\frac{d^2\sigma}{dE d\Omega} \propto \sum_l \left(\frac{\xi}{E_f - E_0} \right)^{\alpha_l} |\langle \phi_{f,l} | e^{i\vec{q}\cdot\vec{r}} | \phi_i \rangle|^2 \rho(E_f), \quad (5)$$

where $\phi_{f,l}$ is the l th partial-wave component of the one-electron final-state wave function near the Fermi energy, with a density of allowed final states $\rho(E_f)$. ϕ_i is the initial one-electron core state and E_0 the threshold energy.

The basic idea is that for small momentum transfer ($q \sim 0$), $e^{i\vec{q}\cdot\vec{r}} \approx 1 + i\vec{q}\cdot\vec{r}$. Thus dipole transitions from the s -like core state to the p -like part of the final state dominate, and the shape of the Li K edge would appear just as in soft-x-ray absorption. As momentum transfer is increased it becomes possible to make monopole transitions from the s core to the s -like part of the final state owing to the increased importance of the next higher term $(\vec{q}\cdot\vec{r})^2$. That is,

$$\frac{d^2\sigma}{dE d\Omega} \propto \left[\left(\frac{\xi}{E_f - E_0} \right)^{\alpha_1} |\langle \psi_{f,1} | e^{i\vec{q}\cdot\vec{r}} | \psi_i \rangle|^2 + \left(\frac{\xi}{E_f - E_0} \right)^{\alpha_0} |\langle \psi_{f,0} | e^{i\vec{q}\cdot\vec{r}} | \psi_i \rangle|^2 \right] \rho(E_f). \quad (6)$$

Doniach *et al.*¹⁸ calculate the one-electron matrix element assuming a hydrogenic-core wave function with a radius of 0.196 Å and a simple OPW final state with a kinetic energy (4.9 eV) about equal to the Fermi energy of a free-electron gas with the density of Li. This value was also chosen for the range parameter ξ . Band structure effects were neglected. Their results showed that at scattering angles equivalent to $q = 3.6 \text{ \AA}^{-1}$ the rounded edge in Li should become completely peaked as at the Na $L_{2,3}$ edge if the final state interactions dominated the threshold region, and thus x-ray scattering should provide a good test of the Mahan-Nozières theory.

The same test can be provided by an inelastic-electron-scattering experiment since the scattering cross section for fast electrons is related to the x-ray scattering cross section by¹⁹

$$\frac{d^2\sigma}{dE d\Omega} \Big|_{\text{electron}} \propto \frac{1}{q^4} \frac{d^2\sigma}{dE d\Omega} \Big|_{\text{x ray}}. \quad (7)$$

Thus at a fixed value of momentum transfer the *shape* of the energy-loss spectrum for inelastic

INELASTIC ELECTRON SCATTERING SPECTROMETER

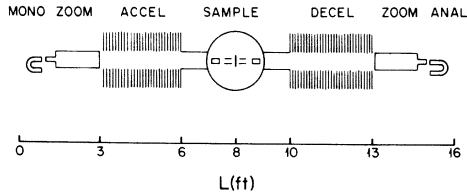


FIG. 1. Inelastic-electron-scattering spectrometer.

electron scattering is identical to that of x-ray inelastic scattering.

II. EXPERIMENT

We have studied the K edge of Li with a newly constructed energy-loss spectrometer shown diagrammatically in Fig. 1. A low-energy highly monoenergetic electron beam is formed in a monochromator designed by Kuyatt and Simpson.²⁰ It is focused onto the thin sample at the center of the apparatus by a zoom lens which is operated at fixed magnification. The scattering angle was selected by deflecting scattered electrons back into the forward direction near the sample with electrostatic deflector plates. This deflection was calibrated by measuring Bragg-scattered electrons. The momentum-transfer resolution function has a FWHM of 0.1 \AA^{-1} . The beam was accelerated to 300 kV, then decelerated and energy analyzed in an analyzer identical to the monochromator. Single electrons were detected in a low-noise (1 count/sec) electron multiplier. Fast electrons which had lost energy E were counted by lowering the pass energy of the monochromator by E volts with respect to the analyzer; then electrons would strike the sample with $300 \text{ keV} + E$ eV kinetic energy. Only those which lost E eV in an inelastic collision with the sample would then be accepted by the analyzer and counted. The measured energy-loss resolution function shown in Fig. 2 has a FWHM of 0.08 eV. With no sample in the beam, the detected intensity was 2×10^{-9} A.

Samples were evaporated *in situ* onto thin formvar or carbon substrates at room temperature. The pressure in the sample chamber was 1.5×10^{-7} Torr before and immediately following evaporation for the room-temperature measurements, and an order of magnitude better for the low-temperature measurements. To achieve low temperatures the sample holder was connected by a copper strap to a nitrogen-temperature cold shield surrounding the sample. Actual sample temperature was estimated by measuring the temperature shift of the plasmon in an Al film held in

an identical sample holder adjacent to the Li sample. The lowest temperature achieved was approximately 160°K . Although sample deterioration in terms of chemically shifted x-ray thresholds became apparent after about 12 h during the room-temperature measurements, no new structure appeared within 3 eV of the x-ray edge, and our data should not be affected in any way by the relatively poor vacuum conditions. All reported data were taken within the first 6 h after evaporation. During evaporation the sample thickness was monitored by observing the intensity of the unscattered main beam, which suffered no energy loss. This beam was attenuated only 5% by the formvar substrate prior to evaporation. Enough lithium was evaporated to reduce the transmission to $1/e$ of its original value. This thickness produces the maximum counting rate for single-scattering events. In the forward scattering direction ($q \sim 0$) the counting rate was about 35 000 counts/sec at threshold, whereas at $q = 1.2 \text{ \AA}^{-1}$ (the first Brillouin zone boundary) the rate was 150 counts/sec. This large decrease is due to the $1/q^2$ dependence of the cross section and is an inherent problem in electron scattering. Data were not taken at greater values of momentum transfer so as to avoid the possibility of umklapp processes, to keep the noise pulses in the electron multiplier (1/sec) less than 1% of the actual counting rate, and to obtain good statistics in a reasonable amount of time.

Data taking is completely automated. A PDP/8e computer collects and stores the data. It sets the

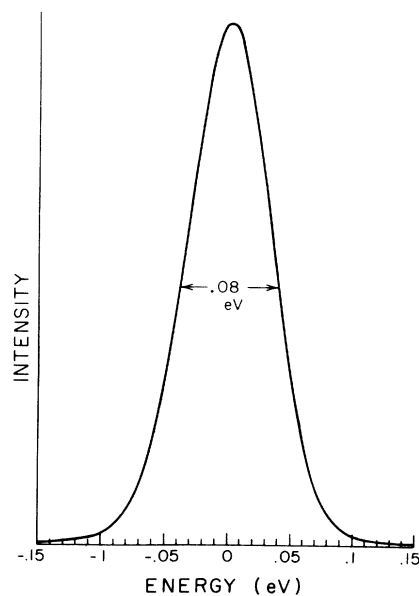


FIG. 2. Measured energy-loss resolution function.

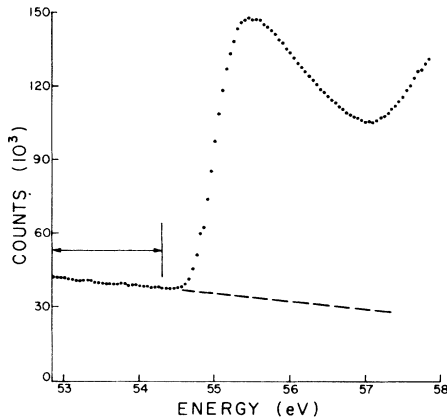


FIG. 3. Raw data, forward scattering: Arrows show background region fit to straight line; dashed line is this straight line extrapolated under absorption edge.

energy loss by programming a digitally programmable power supply which is stable to 30 ppm. The number of pulses from the electron multiplier in a given time interval (usually about 2 sec) is counted by a scalar capable of counting at 100 MHz. The time interval is defined to better than 1 ppm. The computer records the number of counts in a time interval at a particular value of energy loss and then chooses a new energy-loss value and the process is repeated. The range of energy-loss values is scanned many times to average out beam fluctuations, which are generally less than 1%. The total beam intensity may vary by 10% over a period of 12 h. Details of the energy-loss spectrometer will be published elsewhere.²¹

III. DATA ANALYSIS

Data were taken on several different lithium samples prepared as described above, but with slightly different settings of energy and momentum resolution. Although the data reported here is for one particular sample, it is completely reproducible to within the uncertainty of counting statistics.

Figure 3 shows the energy-loss spectrum for forward scattering ($q \sim 0$) in a region from about 53 to 58 eV measured in steps of 0.05 eV. In the region indicated by arrows (1.5 eV) the background was fit to a straight line by the method of least squares. This line was extrapolated beneath the edge, as shown by the dashed line, and then subtracted from the raw data to produce the reduced data shown in Fig. 4. A similar procedure was used at other values of momentum transfer. Since it was quite apparent that no substantial change in the *shape* of the absorption threshold took place as a function of momentum transfer, we

decided to analyze the data with the aim of putting limits on the various parameters of the Mahan-Nozières theory which might bring that theory into agreement with our experiment. We began by determining in a statistically meaningful way how sensitive our data might be to a change in edge shape. Thus, in producing the data displayed in Fig. 4, we chose an arbitrary scale factor by which to multiply the data at $q = 0.9 \text{ \AA}^{-1}$ and 1.2 \AA^{-1} so as to give best agreement with the data at $q = 0$ by the method of least squares. Such a factor is necessary since the absolute number of counts in the edge was not the same at various values of q .

The shape of the spectrum is in good agreement with the previously measured soft-x-ray absorption edge²²; however, in our data the threshold energy (defined as the energy where absorption is half-maximum) appears shifted about 0.3 eV higher than the synchrotron results. Our measured value of the threshold energy is $55.01 \pm 0.02 \text{ eV}$ at 300°K , and $54.99 \pm 0.02 \text{ eV}$ at 160°K . The reported synchrotron data was taken at 77°K . Since the thermal expansion coefficient approaches zero at low temperature, it does not seem possible that a thermal shift can explain the discrepancy.

This discrepancy is puzzling, particularly since we agree with the DESY²² measurements of $L_{2,3}$ threshold energies in both Na at 33 eV and Al at 72.7 eV, values which bracket the Li energy. We expect our measurement to be extremely precise since it involves merely measuring a very stable voltage to high accuracy.

If our value for the threshold energy is correct, as we believe it to be, then it implies there might be a Stokes shift between the absorption and emission energies. The reported emission energy is 54.7 eV,²³ but Arakawa's recent results indicate a higher energy.²⁴ We feel the resolution of this

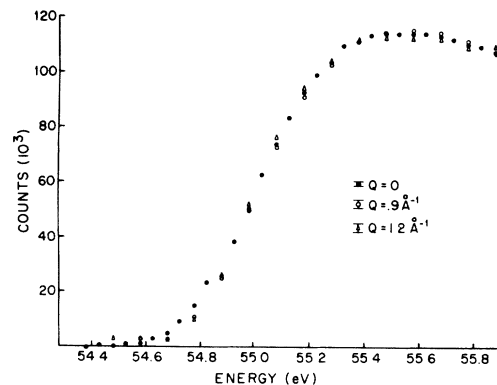


FIG. 4. Momentum-transfer dependence of K absorption edge of Li; all data have been normalized to the data in the forward direction; error bars indicate uncertainty in position of each point due to counting statistics.

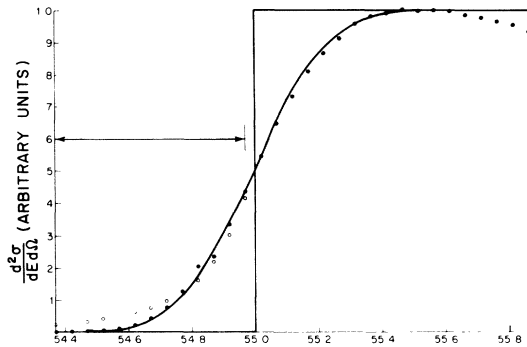


FIG. 5. Determination of broadening function by convolution with step at threshold energy; solid dots are experimental data at $q=0$; solid curve is shape of Gaussian convoluted with step and then with experimental resolution; Gaussian parameters determined by least-squares fit in region between arrows; open circles are best fit to Lorentzian broadening.

question awaits more precise x-ray emission measurements. The existence of a Stokes shift is consistent with a phonon-broadening mechanism of the K -edge energy.

Since there are many parameters involved in describing the threshold shape, it is important to analyze the data carefully to extract as much information as possible. Fortunately, the lifetime broadening of the K edge can be obtained independently of any of the other parameters in the following way: Both competing pictures of the threshold predict an infinite slope at the onset of absorption. Therefore any rounding of the onset can be attributed to a broadening of the threshold energy. We obtained an estimation of the level width by convoluting various broadening functions with a Fermi function for the appropriate temperature at the threshold energy, with height equal to the maximum value above threshold, as illustrated in Fig. 5. The curve shown was obtained by numerically convoluting a Gaussian broadening function of the form

$$f(E) = [(2\pi)^{1/2}\Gamma]^{-1} e^{-E^2/2\Gamma^2}, \quad (8)$$

with a Fermi function at the position of the step function shown and then convoluting the result with our measured energy-loss resolution function of Fig. 2. The parameter Γ was chosen by a least-squares method to match the experimental data at $q=0$ for the lower half of the threshold in the region indicated by arrows. The value of Γ so determined for the room-temperature results was 0.16 ± 0.01 eV, resulting in a broadening function of 0.38 ± 0.02 eV FWHM. If this broadened edge shape is continued beyond the region of the least-squares determination it provides a surprisingly good description of the edge shape, as shown in

Fig. 5. This confirms the previous work of McAlister,¹⁵ who showed that good agreement with experiment could be obtained by convoluting the absorption edge calculated from a one-electron band model with a Gaussian broadening function.

In this analysis our experimental resolution of Fig. 2 contributes about 2% of the final broadening and is nearly negligible. Interestingly enough, our data is much less compatible (in the sense of least-squares differences) with a Lorentzian line broadening of the form

$$f'(E) \propto (E^2 + \Gamma^2)^{-1}. \quad (9)$$

Using a double convolution and least-squares method similar to the previous case we find that for the Lorentzian function $\Gamma \approx 0.12$, and the open circles of Fig. 5 show how Lorentzian broadening fails to match the data before the edge. Several methods for subtracting the background before the edge did not significantly change the data. The same analysis carried out on the samples cooled to 160°K yielded a broadening parameter $\Gamma = 0.15 \pm 0.01$ eV. Therefore, although we do see a sharper edge at lower temperature, most of the sharpening is due simply to a sharper Fermi distribution function. If there is any additional temperature-dependent broadening due to phonons, its contribution to Γ must change by no more than approximately 0.01 eV over the temperature range covered. In what follows we assume that Γ is independent of momentum transfer.

Having obtained a good estimate of the edge broadening function, we calculated the shape of the edge as a function of momentum transfer according to Eq. (5), utilizing the parameters suggested by Doniach *et al.*¹⁸ That is, we used the exponents of Ausman and Glick⁶ and convoluted the theoretical predictions for $q=0$ and $q=1.2 \text{ \AA}^{-1}$ with the broadening function determined as described above. These results are shown in Fig. 6. Since we are only interested in the predicted change in shape we arbitrarily choose to match the theoretical curves at 55.6 eV. Matching the curves closer to threshold would improve agreement near threshold at the expense of greater disagreement further on. Even when appropriately broadened, the theory of final-state electron-hole interactions predicts a dramatic change in shape with momentum transfer. Note also the predicted shift in threshold energy due to broadening the divergent terms. In what follows our units are such that the peak of the absorption at 55.6 eV has been normalized to 1.0.

In the following analysis we varied several possible parameters of the Mahan-Nozières theory in an attempt to show the limits which our experiment places on these parameters. We use as a measure of our sensitivity to shape change the sample stan-

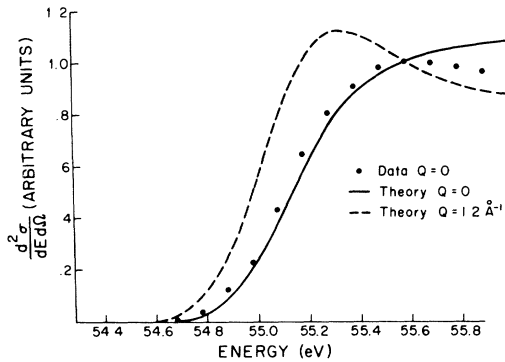


FIG. 6. Predictions of final-state interaction theory; solid curve $q=0$; dashed curve $q=1.2 \text{ \AA}^{-1}$; dots are experimental data at $p=0$.

standard deviation of the data at finite q with respect to the data at $q=0$. We define a spectral difference function

$$D(E_i) = \left. \frac{d^2 \sigma(E_i)}{dE d\Omega} \right|_q - \left. \frac{d^2 \sigma(E_i)}{dE d\Omega} \right|_{q=0}, \quad (10)$$

then the sample standard deviation σ is

$$\sigma = \left[\left(\sum_{i=1}^N [D(E_i)]^2 \right) / (N-1) \right]^{1/2}, \quad (11)$$

where $N (=16)$ is the number of points compared. In Fig. 7 we show the spectral difference between the data at $q=0.09 \text{ \AA}^{-1}$ and $q=1.2 \text{ \AA}^{-1}$ and the forward direction. Also shown is a curve representing the predicted theoretical difference between the spectrum at $q=1.2 \text{ \AA}^{-1}$ and the forward direction according to the Mahan-Nozières theory using the Ausman-Glick parameters. This curve is obtained from Fig. 6. The dashed lines represent

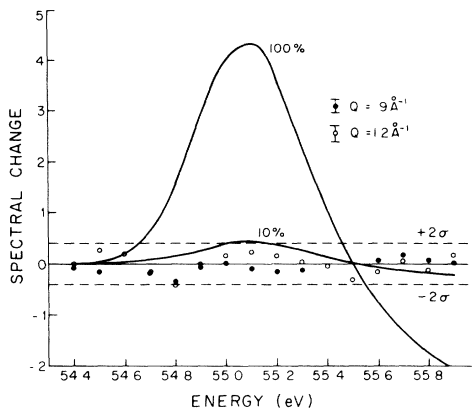


FIG. 7. Difference between experimental spectra at momentum transfer q and $q \approx 0$ (dots). Solid curves are predicted spectral differences in theory of Mahan-Nozières as shown by Doniach *et al.* 100% is present estimation of strength.

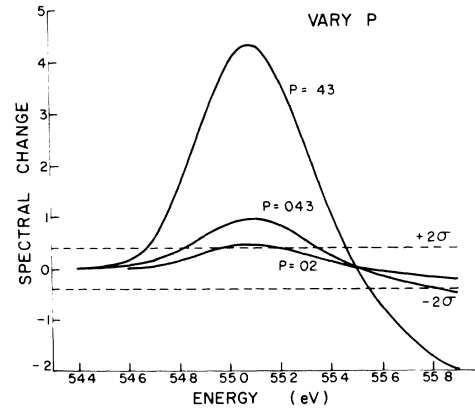


FIG. 8. Effect of varying the s -to- p intensity ratio.

a difference of $\pm 2\sigma$, two standard deviations, from the data at $q=0$. We expect, therefore, to rule out any predicted spectral difference of greater value than 2σ with a confidence level of 90%. Note that the uncertainty due to counting statistics at finite q , indicated by error bars in Fig. 7, results in a standard deviation in good agreement with the sample standard deviation defined above. Also shown in Fig. 7 is a curve indicating that if only 10% or less of the transition strength were influenced by the final-state interaction-theory effects then the predicted spectral difference would lie within our 2σ confidence limit. This possibility, however, is not part of the existing theory.

One possible way of explaining our experimental results without discarding the theory of Mahan and Nozières is for the amount of strength going into the s -wave final state at $q=1.2 \text{ \AA}^{-1}$ to be much smaller than that predicted by Doniach *et al.*¹⁸ One can write the ratio of s -wave to p -wave intensity as a function of q as

$$P(q) = \left| \langle \psi_{f,0} | e^{i\vec{q} \cdot \vec{r}} | \psi_i \rangle \right|^2 / \left| \langle \psi_{f,1} | e^{i\vec{q} \cdot \vec{r}} | \psi_i \rangle \right|^2. \quad (12)$$

In the calculation of Doniach, $P(0)=0$ and $P(1.2 \text{ \AA}^{-1})=0.43$, using the Ausman and Glick exponents and $\xi=4.7 \text{ eV}$ and putting the kinetic energy of the final state equal to 4.7 eV . If the energy of the final state and ξ are taken to be the experimentally determined Fermi energy of lithium, 3.3 eV , then $P(1.2 \text{ \AA}^{-1})=0.66$ and the spectral change should be even greater. Although lithium is a reasonably good free-electron-like metal the simple wave functions used by Doniach may not yield an accurate estimate of P . However, the effect of arbitrarily varying P , shown in Fig. 8, is such that an s -to- p ratio of 2% or more can be excluded by our experiment. It is unlikely that this ratio is less than 2%.

Perhaps a better candidate is the range parameter ξ , taken by Nozières and DeDominicis⁴ to

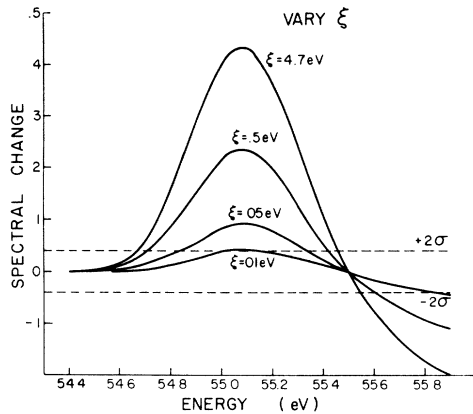


FIG. 9. Effect of varying the range parameter ξ .

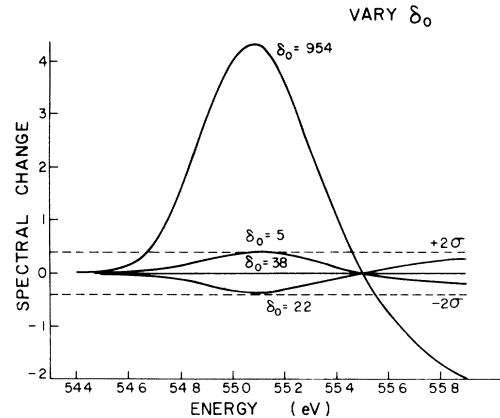


FIG. 11. Effect of varying the s -wave phase shift.

be of the order of the Fermi energy. This parameter was actually calculated by Longe⁸ and shown to be a function of energy with a value always greater than the Fermi energy for absorption processes. As illustrated in Fig. 9, this parameter would have to be less than 0.01 eV to produce a spectral change of less than 2σ between $q=0$ and $q=1.2 \text{ \AA}^{-1}$. Here we have again assumed that $P(1.2 \text{ \AA}^{-1})=0.43$ and that the phase shifts of Ausman and Glick are applicable.

As pointed out in the introduction, the phase shifts for scattering Fermi-surface electrons from the deep core state have been calculated in several models with the predicted values of the s -wave phase shift being between 0.7 and 1.0 rad. Nevertheless, it may be possible that a set of phase shifts can be found which would yield good agreement with our experiment. In the absence of actual model calculations we can make the following estimates. Phase shifts for $l \geq 2$ are inevitably small and could be taken as being zero. Then the s - and p -wave phase shifts are directly related by the Friedel sum rule, Eq. (3), so there is only one free parameter, δ_0 (the s -wave phase shift), which then determines all of the exponents. This method

was suggested by Dow and the curves of Fig. 10 are due to him. A indicates the exponents of Ausman and Glick⁶ and Y the exponents recently suggested by Yue and Doniach.²⁵ We see in Fig. 11 that keeping the accepted values for P and ξ we can vary the s -wave phase shift δ_0 , and find that for $0.22 < \delta_0 < 0.5$ the predicted spectral change lies within our 2σ limits. In fact for $\delta_0=0.38$, $\alpha_0=\alpha_1=0.12$, and there would be absolutely no predicted change with momentum transfer. The region of experimentally acceptable values for the s -wave phase shift is shown by arrows in Fig. 10. In fact our data is only compatible with phase shifts such that $\alpha_1 > 0$, meaning that in the theory of Mahan and Nozières K edges are actually peaked. This means that the observed rounding of the K edges is not due to the Mahan-Nozières theory as has been thought, but to some other broadening mechanism, which is apparently more effective for K edges than L edges. In fact, without any attempts at adjusting parameters such as the threshold, the normalization point (at 55.6 eV), and the density of states above the edge, we show in Fig. 12 that a reasonably good edge shape can be obtained with our previous broadening function and an

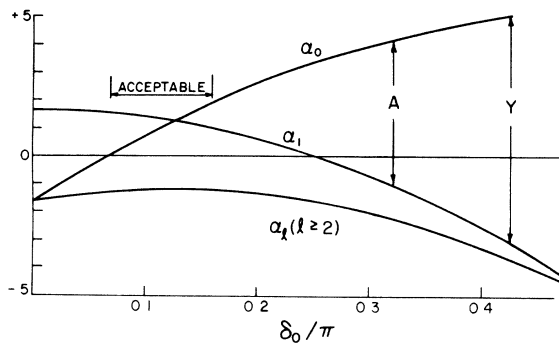


FIG. 10. Exponents as a function of s -wave phase shift.

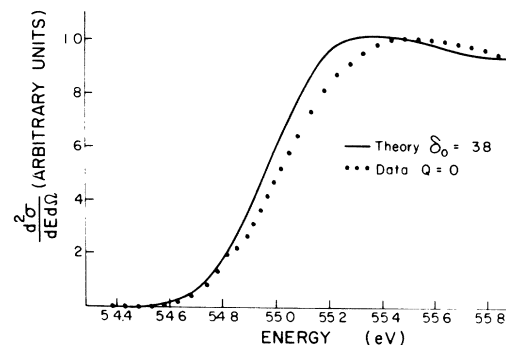


FIG. 12. K edge of lithium with $\alpha_0=\alpha_1=0.2$.

s -wave phase shift of 0.38, which would yield no change in the spectrum with momentum transfer. It is interesting that Longe⁸ has calculated a value of $\delta_0 = 0.53$ for a normal Ashcroft pseudopotential, but he discards that calculation since it does not truly represent the effect of the deep ionized core.

We hasten to point out that the above analysis can not be strictly true for small s -wave phase shifts since then the Friedel sum rule will be dominated by partial waves with $l \geq 2$. In fact, in Fig. 10 one might expect that for any realistic model potential all exponents would approach zero as $\delta_0 \rightarrow 0$, and there would be no region in which $\alpha_0 \approx \alpha_1$ except quite near $\delta_0 = 0$.

IV. CONCLUSIONS

We conclude that the Mahan-Nozieres theory is not important in influencing the shape of the K edge in lithium. The edge is broadened with a Gaussian broadening function with FWHM equal to 0.38 eV. The source of this broadening is yet to be determined, although both Auger decay and coupling to phonons are possibilities. The possible existence of a Stokes shift between emission and absorption spectra has been raised and should be checked by further emission work. We see no evidence for the

predictions of Mahan and Nozières *et al.* which would demand a change in shape of the absorption edge as a function of momentum transfer. By varying, in turn, the individual parameters of the theory of Mahan and Nozières *et al.* and computing the predicted spectral change between the theoretical predictions at $q = 0$ and $q = 1.2 \text{ \AA}^{-1}$, we are able to conclude that one of the following conditions must be met before the theory is deemed compatible with our experiment within 90% confidence limits:

$$\begin{aligned} 0.22 < \delta_0 < 0.5, \\ \xi < 0.01 \text{ eV}, \\ s/p \text{ ratio } (q = 1.2 \text{ \AA}^{-1}) < 0.02, \\ \text{"strength"} < 0.1. \end{aligned}$$

Of course it is possible to vary several parameters so as to restore agreement with our experiment, but such manipulation ought to be theoretically justified.

ACKNOWLEDGMENTS

We gratefully acknowledge the efforts of J. Fields in operating the spectrometer and sincerely appreciate many conversations with J. D. Dow, G. D. Mahan, J. J. Hopfield, T. R. Carver, and P. M. Platzman.

¹G. D. Mahan, Phys. Rev. **163**, 612 (1967).

²B. Roulet, J. Gavoret, and P. Nozières, Phys. Rev. **178**, 1072 (1969).

³P. Nozières, J. Gavoret, and B. Roulet, Phys. Rev. **178**, 1084 (1969).

⁴P. Nozières, and C. T. DeDominicis, Phys. Rev. **178**, 1097 (1969).

⁵J. Fiedel, Philos. Mag. **63**, 153 (1952).

⁶G. A. Ausman and A. J. Glick, Phys. Rev. **183**, 687 (1969).

⁷G. D. Mahan, J. Res. Natl. Bur. Stds. A **74**, 267 (1969).

⁸P. Longe, Phys. Rev. B **8**, 2572 (1973).

⁹G. D. Mahan (private communication).

¹⁰J. D. Dow, J. E. Robinson, and T. R. Carver, Phys. Rev. Lett. **31**, 759 (1973).

¹¹J. D. Dow, Phys. Rev. Lett. **31**, 1132 (1973).

¹²J. D. Dow and B. F. Sontag, Phys. Rev. Lett. **31**, 1461 (1973).

¹³J. D. Dow and D. L. Smith, J. Phys. B **8**, L170 (1973).

¹⁴F. S. Ham, Phys. Rev. **128**, 82 (1962); **128**, 2524

(1962).

¹⁵A. J. McAlister, Phys. Rev. **186**, 595 (1969).

¹⁶B. Bergersen, T. McMullen, and J. P. Carbotte, Can. J. Phys. **49**, 3155 (1971).

¹⁷D. R. Franceschetti and J. D. Dow, Bull. Am. Phys. Soc. **19**, 299 (1974).

¹⁸S. Doniach, P. M. Platzman, and J. T. Yue, Phys. Rev. B **4**, 3345 (1971).

¹⁹D. Pines, *Elementary Excitation in Solids* (Benjamin, New York, 1964), p. 126.

²⁰C. E. Kuyatt and J. A. Simpson, Rev. Sci. Instrum. **38**, 103 (1967).

²¹S. E. Schnatterly, P. C. Gibbons, and J. J. Ritsko (unpublished).

²²R. Haensel, G. Keitel, B. Sonntag, C. Kunz, and P. Schrieber, Phys. Status Solidi **2**, 85 (1970).

²³T. Sagawa, in *Soft X-ray Band Spectra*, edited by D. J. Fabian (Academic, New York, 1968), p. 29.

²⁴E. T. Arakawa (private communication).

²⁵J. T. Yue and S. Doniach, Phys. Rev. B **8**, 4578 (1973).